

Origin of ultraviolet luminescence from bulk ZnO thin films grown by molecular beam epitaxy

M. Asghar^{1, a}, Khalid Mahmood^{1, b}, Adnan Ali^{1, c}, M-A Hasan^{2, d}, I. Hussain^{3, e}, M. Willander^{3, f}

¹ Physics department, The Islamia University of Bahawalpur, Pakistan

² Department of Physics and Optical Sciences, Charlotte NC 28223, USA

³ IFM, Linköping University 58183 Linköping, Sweden

^amhashmi@iub.edu.pk, ^bkhalid_mahmood856@yahoo.com, ^cadnan_1982@yahoo.com,

^dmhasan@uncc.edu, ^eijaas@itn.liu.se, ^fmagnus.willander@itn.liu.se,

Keywords: ZnO thin films; Energy dispersive x-ray spectroscopy; Zn-interstitial; X-ray diffraction Photoluminescence; Raman spectroscopy

Abstract. Origin of ultraviolet (UV) luminescence from bulk ZnO has been investigated with the help of photoluminescence (PL) measurements. Thin films of ZnO having 52%, 53% and 54% of Zn-contents were prepared by means of molecular beam epitaxy (MBE). We observed a dominant UV line at 3.28 eV and a visible line centered at 2.5 eV in the PL spectrum performed at room temperature. The intensity of UV line has been found to depend upon the Zn percentage in the ZnO layers. Thereby, we correlate the UV line in our samples with the Zn-interstitials-bound exciton (Zn_i-X) recombination. The results obtained from, x-ray diffraction, the energy dispersive X-ray spectrum (EDAX) and Raman spectroscopy supported the PL results.

Introduction

ZnO is one of the most attractive materials of today's research due to its mechanical, electrical, optical, magnetic and spintronic applications [1, 2]. ZnO is especially preferred on the rest of the optical materials due to its tri-luminescence properties: green/blue, violet and UV [3, 4]. Above all, UV emission from ZnO has brought it in the front line of the biomaterials to be used as biosensors and/or bacteria killers [5]. But the effectiveness of the device is of course, dependent on its quantum efficiency. As of today, oxygen vacancies and zinc vacancies are known as the sources of green and violet luminescence from the ZnO, respectively [6, 7]. But UV emission at room temperature from ZnO has been attributed to several origins: for example, Vladimir et al.[8] assigned the recombination of donor-bound exciton with UV emission from ZnO where donor entity was not identified, Yang Zhang et al.[9] referred the UV peak as free exciton recombination process; Reynolds et al.[10] correlated it with an acceptor related transition, Ü. Özgür et al.[11] and L.L. Yang et al.[12] identified UV luminescence as acceptor-bound-exciton and surface band bending of ZnO, respectively. These scattered and unclear results are not sufficient to ascertain the real origin of UV emission from ZnO, and hence the interest is continued amongst the researchers.

In this paper the origin of ultraviolet (UV) luminescence from bulk ZnO has been investigated with the help of photoluminescence (PL) measurements performed at room temperature. A dominant PL peak at 3.28 eV is found in all samples but the PL intensity is higher in the sample having higher Zn-contents. Thereby we correlate the observed PL peak with Zn interstitials-bound exciton recombination. X-ray diffraction (XRD), Raman scattering and energy dispersive x-ray spectroscopy (EDAX) have been additionally employed which support the PL results.

Experimental

ZnO has hexagonal structure where all the octahedral sites in ZnO are empty. These empty sites are occupied preferably by the rich contents and/or point defects during the growth. Keeping this aspect of ZnO structure in view, we deliberately set the growth condition such that Zn-contents in the

Table. 1 Substrate temperature, Zn-cell temperature, time of growth, pressure of growth and thickness of sample A, B and C.

Sample ID	T _{Sub.} (°C)	T _{Zn-Cell} (°C)	Time of growth (Hrs)	P _{growth} (torr)	Thickness (μm)
A	410	276	9	1×10^{-4}	1.5
B	420	282	8	1×10^{-4}	1.3
C	430	289	7	1×10^{-4}	1.0

Samples should be purposefully higher. Three layers of bulk ZnO each having thickness 1.5, 1.3 and 1 micron (hereafter referred as A and B and C) were grown on 3 inch diameter p-type silicon (111) wafers by means of molecular beam epitaxy (MBE). The growth conditions within 0.5% tolerance for samples A, B and C can be seen in Table. 1. EDAX measurements were performed to verify the composition of the as-grown A, B and C layers. Accordingly the atomic % of Zn contents in A, B and C layers were found to be 52%, 53% and 54%, respectively. Characterization of ZnO films were carried out by the following equipment: PL and Raman spectroscopy by Horiba using He-Cd laser of excitation wavelength 325 nm, XRD by PANALytical X'pert and SEM/EDAX by JEOL. All the measurements were performed at room temperature.

Results and discussion

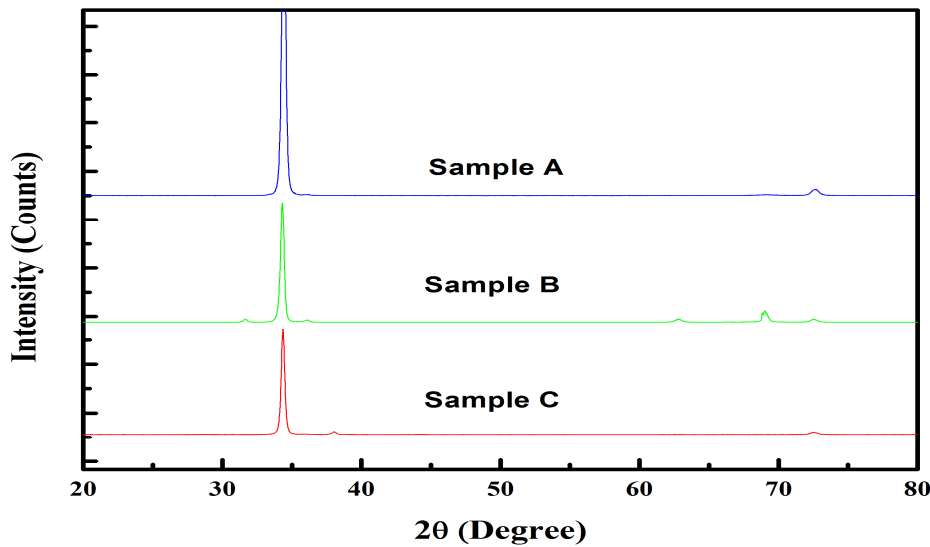


Fig. 1 X-ray diffraction pattern of ZnO lattice structure. A dominant peak corresponding to (002) plane in sample A, B and C indicates polycrystalline growth along (002) plane.

XRD patterns of the as grown samples A, B and C confirmed hexagonal structure of ZnO (see Fig. 1). All samples exhibited three distinct peaks at angles (2θ): 34.47° , 36.2° and 72.4° corresponding to the (002), (101) and (004) planes of ZnO, respectively [13]. Peak (002) being the dominant among the others, indicates that the preferable direction of the growth is along this plane i.e. *c*-plane. The full width at half maximum (FWHM) for (002) peak for sample A, B and C is 0.30° , 0.32° and 0.35° respectively, which indicates that sample A has better microstructure as compared to sample B and C [14]. Similarly, the grain sizes, calculated by Scherrer's formula: 26 nm, 24 nm and 22 nm for sample A, B and C, respectively. This means that the higher values of Zn-concentration in the samples decrease the crystallinity of layers.

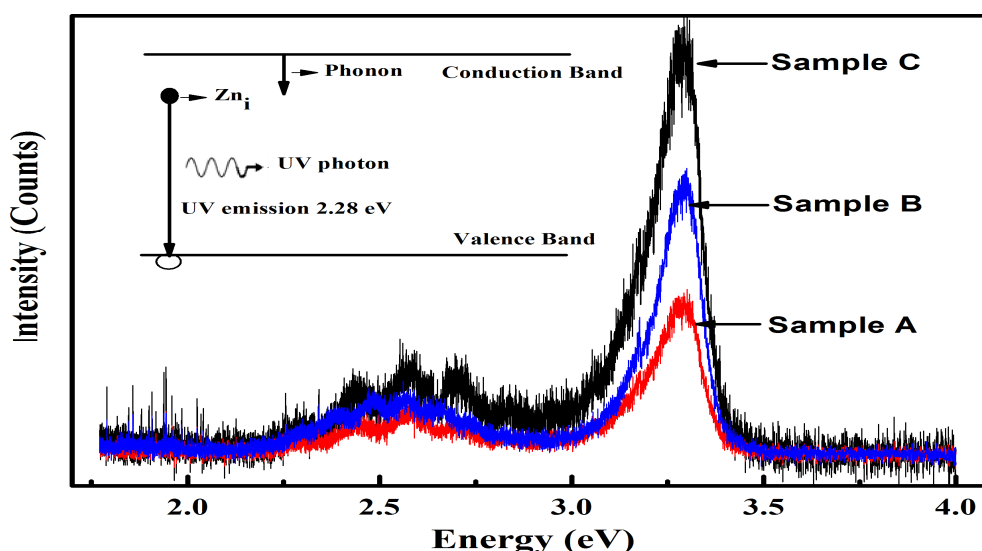


Fig. 2 Comparative PL spectra of sample A, B and C taken at room temperature, visible and UV emission related peaks are prominent in all samples. Inset explains the UV emission process in the ZnO.

Fig. 2 demonstrates room temperature PL spectra of samples A, B and C measured by 325 nm laser source. To avoid the excitation intensity effect in the PL spectra, [15] the incident intensity of the laser source was kept constant for all samples measurements. In the Fig 2, we observed a strong UV peak at 3.28 eV and a broad band in range of 2.36 eV - 2.67 eV centered at 2.5 eV. As per information from the literature, the broad band is attributed to green/blue luminescence. The source of this luminescence is identified as oxygen vacancies [3]. The intensity of UV peak associated with sample C is almost three times than that of sample A. Since the PL intensity of the broad band observed in samples A, B and C is the same, the variation of existing UV peaks can therefore be proportionally related with the concentration of recombination-generation centers. A number of reports can be seen in the literature demonstrating the UV emission from ZnO [8-12]. In view of the results reported in references [8-12], it is clear that UV emission is qualitatively related with bound exciton-donor transition. But nevertheless, PL is an elegant and nondestructive technique to characterize the radiative point defects in the band gap of the material, but, none of the foresaid reports categorically speaks about correlation of such defects with their PL results. Keeping this significant discrepancy in the literature in view, we focused on the native defects in ZnO to justify 3.28 eV line in our PL results. Therefore in the following we will discuss the role of Zn_i associated with 3.28eV peak.

ZnO has hexagonal structure with all the tetrahedral sites are equally occupied by Zn and O atoms but all the octahedral sites are essentially empty, hence there are a plenty of sites for ZnO to accommodate the defects like Zn-interstitials, O-vacancy and/or Zn-antisite, intrinsically and/or extrinsically [16]. Under Zn vapor rich environments Zn interstitials are known to be dominant intrinsic donor defects in bulk ZnO [17]. The thermal activation energy of the Zn_i lies in the range of 0.02 eV – 0.2 eV below the minimum of conduction band edge as determined by electrical techniques as well as theoretical calculations [18, 19]. Zn_i being ionized donor sites below the conduction band at room temperature, act as effective electron traps. The major evidence of this argument follows the n-type conductivity of the material. When a laser beam having energy greater than band gap, is incident on the sample, electrons from the valance band (leaving hole behind) travel to conduction band but are trapped by ionized Zn-interstitial defects located below the conduction band minimum edge. Due to constant temperature, Fermi level is pinned below the ionized states therefore, the trapped carriers must be re-emitted from the traps and subsequently they recombine at the holes states in valence band edge. As a result, photons of energy 3.28 eV are emitted to give out UV luminescence and also phonon of energy 0.09 eV from ZnO layers ($E_g=3.37$ eV).

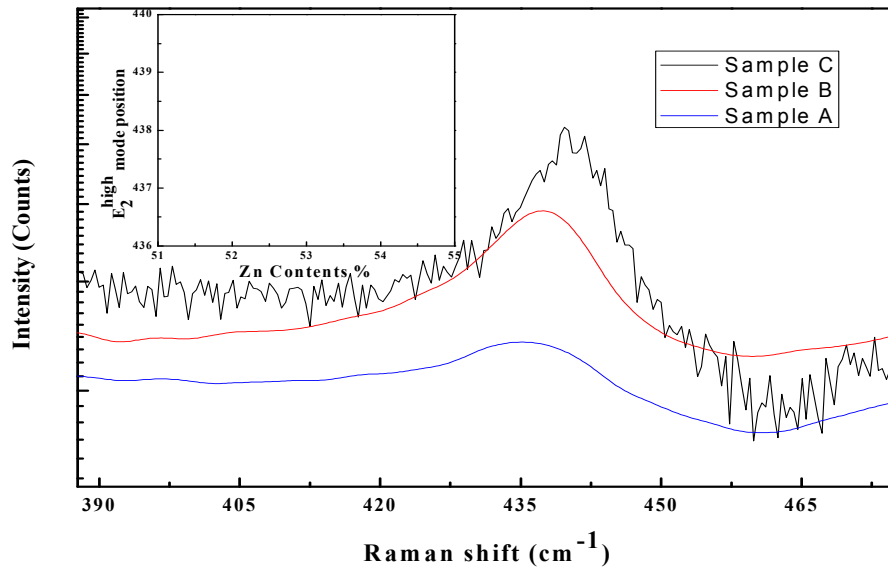


Fig. 3 Raman spectrum of samples A, B and C demonstrate ZnO associated non-polar (E_2^{high}) and polar $E_1(\text{LO})$ modes. The experimental values exhibit shift from the theoretical values: 433 and 574 cm^{-1} , respectively. The upward shift in E_2^{high} is attributed to the presence of Zn-interstitials [4].

To support our PL results, we performed Raman spectroscopy as well. The ZnO crystal structure belongs to the space group C_{6v}^4 , and the group theory analysis predicts the zone-center optical modes; $A_1 + 2B_1 + E_1 + 2E_2$ (E_2^{low} , E_2^{high}). The A_1 , E_1 and the two E_2 are Raman active modes, while the B_1 modes are forbidden in Raman scattering. A_1 and E_1 modes are polar: their vibrations polarize the unit cell, which results in the creation of a long-range electrostatic field. This field results in the splitting of A_1 and E_1 modes into longitudinal optical (LO) and transverse optical (TO) components, thus creating the $A_1(\text{LO}, \text{TO})$ and $E_1(\text{LO}, \text{TO})$ modes. However, their observation is subject to the incident angle of laser and orientation of the layer.

Fig 3 displays Raman spectra of samples A, B and C measured at room temperature using excitation laser 325 nm. We observed E_2^{high} mode at 437 cm^{-1} , 438 cm^{-1} and 439.5 cm^{-1} for sample A, B and C, respectively. The theoretical calculations by Tsuboi and Wada predicted the frequency of E_2^{high} mode of pure ZnO to be 433 cm^{-1} [20]. Huang et al. [21] pointed out that the excess of Zn-interstitials in the films shifts the E_2^{high} upward. In this perception the observed upward shifts in E_2^{high} frequency in samples A, B and C is correlated with the relative volume of Zn-interstitials therein and hence support the PL results.

Summary

In conclusion, we have investigated the origin of UV emission from Zn-rich ZnO, prepared by molecular beam epitaxy with different thicknesses. Using PL technique, it is found that the origin of UV emission from ZnO is in fact, related with Zn-interstitials. The remarkable increase in the intensity of UV emission was observed with the increase of Zn contents in samples. Our results demonstrate that UV emission can be enhanced by growing ZnO in Zn-rich conditions. EDAX and Raman data effectively supported our results.

Acknowledgement

Authors are thankful to Higher Education Commission Pakistan for financial support under project No. 1019/R&D. The authors are also thankful to UNC-Charlotte, USA for technical support.

References

- [1] C.W. Zou, H.J. Wang, M.L. Yi, M. Li, C.S. Liu, L.P. Guo, D.J. Fu, T.W. Kang, Defect related room temperature ferromagnetism in p-type (Mn, Li) co-doped ZnO films deposited by reactive magnetron sputtering, *Appl. Surf. Sci.* 256 (2010) 2453.
- [2] N. Bano, I. Hussain, O. Nur, M. Willander, Q. Wahab, A. Henry, H.S. Kwack, D. Le Si Dang, Depth resolved cathodoluminescence study of Zinc Oxide nanorods catalytically grown on p-type 4H-SiC, *J. Lumin.* 130 (2010) 963-969.
- [3] K. Prabakar, Choongmo Kim, Chongmu Lee, *Cryst. Res. Technol.* UV, violet and green/blue luminescence from RF sputter deposited ZnO:Al thin films, 40 (2005) 1150.
- [4] H.A. Ahn, Y.Y. Kim, D.C. Kim, S.K. Mohanta, H.K. Cho, A comparative analysis of deep level emission in ZnO layers deposited by various methods, *J. Appl. Phys.* 105 (2009) 013502.
- [5] Jae-Hong Lim, Chang-Ku Kang, Kyoung-Kook Kim, Il-Kyu Park, Dae-Kue Hwang, Seong-Ju Park, UV electroluminescence from ZnO light-emitting diodes grown by high-temperature radiofrequency sputtering, *Adv. Mater.* 18 (2006) 2720 – 2724
- [6] L. M. Wong, S. Y. Chiam, J. Q. Huang, S. J. Wang, J. S. Pan, W. K. Chim, Role of oxygen for highly conducting and transparent gallium-doped Zinc Oxide electrode deposited at room temperature, *Appl. Phys. Lett.* 98(2011) 022106.
- [7] B.D. Ngom, O. Sakho, N. Manyala, J.B. Kana, N. Mlungisi, L. Guerbous, A.Y. Fasasi, M. Maaza, A.C. Beye, Structural, morphological and photoluminescence properties of W-doped ZnO nanostructures, *Appl. Surf. Sci.* 255 (2009) 7314-7318.
- [8] Vladimir A Fonoberov, Khan. A. Alim, Alexander A. Balandin, Faxian Xiu, Jianlin Liu, Photoluminescence investigation of the carrier recombination process in ZnO quantum dots and nanocrystals, *Phys. Rev. B* 73 (2006) 165317.
- [9] Yang Zhang, Bixia Lin, Zhuxi Fu, Cihui Liu, Wei Han, Strong ultraviolet emission and rectifying behavior of nanocrystalline ZnO, *Optical Mater.* 28 (2006) 1192-1196.
- [10] D. C. Reynolds, D. C. Look, B. Jogai, R. L. Jones, C. W. Litton, H. Harsch, G. Cantwell, Optical properties of ZnO crystal containing internal strain, *J. Lumin.* 82 (1999) 173.
- [11] Ü. Özgür, Ya. I. Alivov, C. Liu, A. Teke, M. A. Reshchikov, S. Doğan, V. Avrutin, S.-J. Cho, H. Morkoç, A comprehensive review of ZnO materials and devices, *J. Apply. Phys.* 98 (2005) 041301.
- [12] L. L. Yang, Q. X. Zhao, M. Q. Israr, J. R. Sadaf, M. Willander, G. Pozina, and J. H. Yang, Indirect optical transition due to surface band bending in ZnO nanotubes, *J. Appl. Phys.* 108 (2010) 103513.
- [13] S.S. Tneh, Z. Hassan, K.G. Saw, F.K.Yam, H.Abu Hassan, The structural and optical characterization of ZnO synthesized using bottom-up growth method, *Physica B* 405 (2010) 2045.
- [14] X. Wang, Y.M. Lu, D.Z. Shen, Z.Z. Zhang, B.H. Li, B.Yao, J.Y. Zhang, D.X. Zhao, X.W. Fan, growth and photoluminescence for undoped and N-doped ZnO grown on 6H-SiC substrat, *J. lumin.* 122 (2007) 165-167.
- [15] R. Sing, R. J. Molnar, M. S. Unlu, T.D. Moustakas, *Apply. Phys. Lett.* (3) 64 (1994) 17.
- [16] Lukas Schmidt-Mende, Judith L. MacManus-Driscoll, ZnO-nanostructures, defects, and devices, *Materialstoday* 10 (2007) 40.
- [17] D. Behera, B.S. Acharya, Nano-star formation in Al-doped ZnO thin film deposited by dip-dry method and its characterization using atomic force microscopy, electron probe microscopy, photoluminescence and laser Raman spectroscopy, *J. Lumin.* 128 (2008) 1577-1586.
- [18] D. C. Oh, T. Suzuki, J. J. Kim, H. Makino, T. Hanada, M. W. Cho, T. Yao, Electron-trap center in ZnO layers grown by molecular-beam epitaxy, *Appl. Phys. Lett.* 86 (2005) 032909.
- [19] M. Fox, *Optical properties of solids*, Oxford University press, New York, 2001.
- [20] M. Tsuboi, A. Wada, Optically active lattice vibrations in Wurtzite-type crystals of Zinc Oxide and Cadmium Sulfide, *J. Chem. Phys.* 48 (1968) 2615.
- [21] Yanqiu Huang, Meidong Liu, Zhen Li, Yike Zeng, Shaobo Liu, Raman spectroscopy of ZnO based ceramic films fabricated by novel Sol-gel process, *Mater. Sci. Eng B.* 97 (2003) 111.